(2)

TECHNICAL REPORT BRL-TR-3365

BRL

A BOUNDARY INTEGRAL APPROACH FOR THREE-DIMENSIONAL UNDERWATER EXPLOSION BUBBLE DYNAMICS

STEPHEN WILKERSON

JUNE 1992

U.S. ARMY LABORATORY COMMAND

BALLISTIC RESEARCH LABORATORY
ABERDEEN PROVING GROUND, MARYLAND

NOTICES

Destroy this report when it is no longer needed. DO NOT return it to the originator.

Additional copies of this report may be obtained from the National Technical Information Service, U.S. Department of Commerce, 5285 Port Royal Road, Springfield, VA 22161.

The findings of this report are not to be construed as an official Department of the Army position, unless so designated by other authorized documents.

The use of trade names or manufacturers' names in this report does not constitute indorsement of any commercial product.

REPORT DOCUMENTATION PAGE

Form Approved
OMB No. 0704-0188

1. AGENCY USE ONLY *(Leave blank)*	2. REPORT DATE	3. REPORT TYPE AND DATES COVERED
	June 1992	Final, November 1989–June 1990

4. TITLE AND SUBTITLE

A Boundary Integral Approach for Three-Dimensional Underwater Explosion Bubble Dynamics

5. FUNDING NUMBERS

1L162618AH80

6. AUTHOR(S)

Stephen Wilkerson

7. PERFORMING ORGANIZATION NAME(S) AND ADDRESS(ES)

8. PERFORMING ORGANIZATION REPORT NUMBER

9. SPONSORING/MONITORING AGENCY NAME(S) AND ADDRESS(ES)

U.S. Army Ballistic Research Laboratory
ATTN: SLCBR-DD-T
Aberdeen Proving Ground, MD 21005-5066

10. SPONSORING/MONITORING AGENCY REPORT NUMBER

BRL-TR-3365

11. SUPPLEMENTARY NOTES

12a. DISTRIBUTION/AVAILABILITY STATEMENT

Approved for public release; distribution is unlimited.

12b. DISTRIBUTION CODE

13. ABSTRACT *(Maximum 200 words)*

The development of a numerical solution for three-dimensional underwater explosion bubble dynamics using the Boundary Integral Method is presented. Using the boundary integral phenomenology, computer programs have been developed and some results are presented. Future improvements to the existing code to extend its applicability for parametric bubble dynamics studies are given.

14. SUBJECT TERMS

explosion bubbles; cavitation; underwater explosion; boundary element; boundary integral method

15. NUMBER OF PAGES

34

16. PRICE CODE

17. SECURITY CLASSIFICATION OF REPORT	18. SECURITY CLASSIFICATION OF THIS PAGE	19. SECURITY CLASSIFICATION OF ABSTRACT	20. LIMITATION OF ABSTRACT
UNCLASSIFIED	UNCLASSIFIED	UNCLASSIFIED	SAR

INTENTIONALLY LEFT BLANK.

TABLE OF CONTENTS

INTENTIONALLY LEFT BLANK.

LIST OF FIGURES

INTENTIONALLY LEFT BLANK.

ACKNOWLEDGMENTS

The author wishes to thank Dr. Minos Moussouros, Dr. George Chahine, and Professor Andrea Prosperetti for their continued help and patience that enabled this study to be completed. The author also gratefully acknowledges the support of the U.S. Army Ballistic Research Laboratory (BRL), Aberdeen Proving Ground, MD, in making the preparation of this manuscript possible.

INTENTIONALLY LEFT BLANK.

1. INTRODUCTION

The work presented considers the adaptation of potential theory and the boundary integral method for the development of computer codes to simulate underwater explosion bubble dynamics. In order to understand the development of numerical methods like this, it is important to review some of the pioneering efforts which have lead to its use. One of the early studies in the area of bubble dynamics was published by Benjamin and Ellis (1966). Much of the work that followed builds from this fundamental study. Benjamin and Ellis' work provided a broad examination of the subject matter referring to the well-known implosion mechanism first recognized by Lord Rayleigh (1917). Their study included a review of the contributions of such notable authors as Taylor (1950), Taylor and Davies (1950), Cole (1948), Lamb (1945), Knapp and Hollander (1948), Knapp (1958a, 1958b), and Hammitt (1963). The effort also provided insight into the physics of bubble jetting. In doing so, the mechanisms leading to bubble collapse and jetting were examined from both a physical and mathematical standpoint. In their presentation, the authors considered the importance of the Kelvin impulse. The bubble's impulse was used to explain the nature of bubble collapse, jetting, and the formation of toroidal bubbles. They explained, "As a general interpretation of the phenomenon of jet penetration through collapsing cavities, one can simply say that the liquid is finding the only possible way to preserve its impulse as the cavity size decreases." After a thorough overview of the bubble pulsation and jetting phenomenon, the authors proceeded to investigate the phenomenon through a series of experiments. The primary concern of their study was with the small-scale hydrodynamic processes that lead to cavitation damage. Therefore, the experimental investigation was initiated with the aim of examining the phenomena of bubble collapse and jetting near rigid bodies. In the experiments, a free-fall apparatus was used which created a gravity-free environment to observe bubble collapse. Additionally, by holding the experimental apparatus fixed, the effects of gravity on bubble collapse were observed. Using this device, the effects of a nearby boundary and gravity on bubble jetting were observed separately. The results provided conclusive proof of bubble jetting in the free field, due to gravity, as well as bubble jetting influenced by a nearby rigid wall.

Studying the same phenomena, Plesset and Chapman (1971) developed numerical techniques designed especially for the calculation of bubble collapse and jetting near rigid

boundaries. In this model, the effects of viscosity and compressibility of the fluid were neglected in the basic conservation laws for mass and momentum. A number of other simplifying assumptions were made in their model. In summary, they are as follows:

(1) The liquid is incompressible.
(2) The flow is inviscid.
(3) The vapor pressure inside the bubble is uniform and constant.
(4) The ambient fluid pressure remains constant with time.
(5) The bubble contains no permanent gas.
(6) Surface tension effects are negligible.
(7) The effects of gravity are not included.
(8) The bubble is initially spherical and remains axisymmetric thereafter.

As pointed out in their paper, only the first three assumptions are essential to the method developed. Correspondingly, the same three initial assumptions are adopted in the current study. Under the assumptions used in their model, the velocity is equal to the gradient of a potential which satisfies Laplace's equation, and the pressure is given by Bernoulli's equation. The analysis was carried out based on these equations and a finite difference integration scheme. In their investigation, Plesset and Chapman simulated two specific cases of an initially spherical bubble collapsing near a plane solid wall. Their calculation predicted bubble jet speeds sufficient to explain cavitation damage.

In a related numerical study, Chapman and Plesset (1972) extended their original calculations to include vapor bubbles in an infinite liquid initially perturbed from the spherical shape. In this study, two cases of bubble collapse were simulated, namely, an oblate ellipsoid and a prolate ellipsoid. The calculations showed the formation of a high-speed bubble jet during the late stages of bubble collapse. In both calculations, the bubble's initially elliptical shape was transformed into a dumbbell shape in the opposite direction of the original elongation during the bubble's collapse. The results also showed the important point—that a very small, initial deformation from a spherical shape limits the applicability of the assumption of spherical symmetry. One final important point was that the analysis indicated that the jet speed at the time of impact is smaller than had been found using linearized theories.

Another theoretical study important to bubble dynamics was presented by Blake and Gibson (1981). In their numerical approach, they proceeded under the same fundamental assumptions of Plesset and Chapman (1971) using incompressible, irrotational flow and a uniform, internal bubble pressure. The solution centered around the use of a number of ring distributions of singularities to calculate the potential. The new method was physically more appropriate than previous methods based on line distributions (Bevir and Fielding 1974). In their paper, Blake and Gibson investigated the damaging effects of cavitation bubbles and methods to reduce the possibility of cavitation damage. As pointed out in their work and from the law of Bjerknes, oscillating bubbles tend to migrate toward rigid boundaries and away from a free surface. Furthermore, the migration and jetting of bubbles near flexible boundaries are not fully understood. Their investigation into flexible surfaces concentrated around both numerical and experimental studies using spark-generated bubbles near a free surface—a free surface being the limit of flexible surfaces. The study revealed that the approximate integral-equation approach presented was adequate to simulate the growth and collapse of vapor bubbles at least one maximum bubble radius from the free surface. They additionally observed that vapor bubbles in the absence of gravity can be generated within half a maximum radius of the free surface without venting. Their work provided some excellent photography and insight into the behavior of bubbles near a free surface.

An alternate numerical approach which was published around the same time as the Blake and Gibson (1981) contribution and was written by Guerri, Lucca, and Prosperetti (1980). Their method entailed the use of the now-familiar boundary integral numerical method for the simulation of nonspherical cavitation bubbles in inviscid, incompressible liquids. Their work offered an attractive alternative to the finite difference (Plesset and Chapman 1971), perturbation (Chapman and Plesset 1972; Chahine 1977), and singularity (Blake and Gibson 1981) methods that had been previously presented. The crucial step in the procedure involves the solution of the potential problem. The potential solution is found using the boundary integral or boundary element method which is based on an exact relation, namely, Green's identity. One of the more attractive features of their approach is the method's efficiency. The efficiency comes from the need of only surface values for the velocity potential and its first derivative. Therefore, the method avoids the problem of solving Laplace's equation over the entire domain occupied by the liquid. Another appealing feature of the boundary integral method is its excellent performance in calculating the unstable collapse

phase of the bubble without smoothing techniques. In order to show the reliability of the computational model, one of the cases originally studied by Plesset and Chapman was considered for comparison. In this comparison, the velocities of the bubble jet tip agreed favorably with the previous calculations of Plesset and Chapman. The results presented several examples of the method's capability to predict bubble collapse and jetting in axisymmetric configurations. They included the collapse of a bubble near a rigid wall, as previously studied by Plesset and Chapman, and the calculation of bubble collapse for three bubbles with colinear centers. Their method was crucial for future multidimensional bubble codes.

Another major contribution in the field of bubble dynamics was presented by Chahine, Perdue, and Tucker (1988). Their work introduced, for the first time, an economical approach to the numerical study of three-dimensional (3-D) bubble dynamics. The essence of the method was based on the boundary integral approach. Nonetheless, their study revealed a number of limiting factors in the boundary integral approach's applicability for 3-D bubble dynamics, as well as a number of solutions to unforeseen problems in the method. Their work required a number of contributions in the process of developing numerical methods to simulate underwater explosion bubble dynamics. One of the hurdles that Chahine and Perdue needed to overcome was the calculation of the boundary integral method's surface integrals in 3-D configurations. Originally, the numerical calculation of these integrals was thought too formidable for simple numerical approximation. Therefore, Perdue (1988) underwent the laborious task of calculating the integrals out exactly. Chahine and Perdue also devised some innovative methods for the calculation of the tangential components of velocity on the surface of the bubble. In all these approaches, a number of unforeseen problems with 3-D boundary integral techniques arose. They included geometric perturbations caused by the choice of the initial grid, solid angle calculations, initial geometries, and numerical instabilities, to mention only a few. In Chahine and Perdue's report on the approach, they focused on explosion bubbles as their topic of interest and discussed the application of their work in calculating bubble collapse near submerged bodies. They also presented a number of calculations with rigid plates at various angles of inclination, a calculation near a submerged body, and some axisymmetric calculations. Their work represented a significant contribution in the field of computational bubble dynamics. Their work additionally offered a springboard into numerous unanswered questions regarding the boundary integral method and 3-D computational models.

2. MATHEMATICAL DEVELOPMENT

The first step in the formulation of this bubble dynamics model was to put the basic laws of nature governing the phenomenon into a suitable mathematical form. The physical conditions imposed on the model are depicted graphically in Figure 1. The fluid occupies a domain Ω, bounded by the bubble surface, S_b, solid boundaries, S_r, and a surface at infinity, S_∞. The fluid contained in the domain Ω is considered incompressible, and inviscid flow is also assumed. Furthermore, the gas in the bubble is assumed adiabatic. In order to justify these assumptions, the physical nature of an underwater explosion bubble must be considered. In the case of underwater explosive detonations, a chemical reaction converts the original material very quickly into a gas at a very high temperature and pressure. The temperature of the explosive products directly after detonation can be of the order of 3,000° C, with pressures on the order of 50,000 mpa (Cole 1948). The result of the initial detonation is a compression or shock wave being emitted into the fluid field, followed by the dynamic expansion and contraction of the gaseous products. After the release of the shock wave, which is an early time phenomenon, the speed of the bubble's surface remains at least an order of magnitude smaller than the speed of sound in water. Therefore, the imposition of an incompressible condition on the fluid is deemed valid for this flow after the first few microseconds.

Using the bubble radius in the expansion or contraction phase of the bubble pulse as a characteristic length, a Reynolds number can be calculated. This Reynolds number is found to be high through most of the bubble growth and collapse. Recalling that the Reynolds number is the ratio of inertial to viscous forces, it is clear that neglecting viscous terms in the conservation of momentum equation detracts very little from the accuracy of the solution. Additionally, under the assumptions that the fluid flow is inviscid and irrotational, the velocity field can be found from Laplace's equation. In the case of a cavitation bubble, similar assumptions were shown to be valid by Guerri, Lucca, and Prosperetti (1980) and others (Blake, Taib, and Doherty 1986; Chahine 1982; Oguz and Prosperetti 1989). In summary, the gradient of the potential normal to a rigid body is zero, the potential can be determined on the bubble surface initially, and the velocity and potential at infinity vanish.

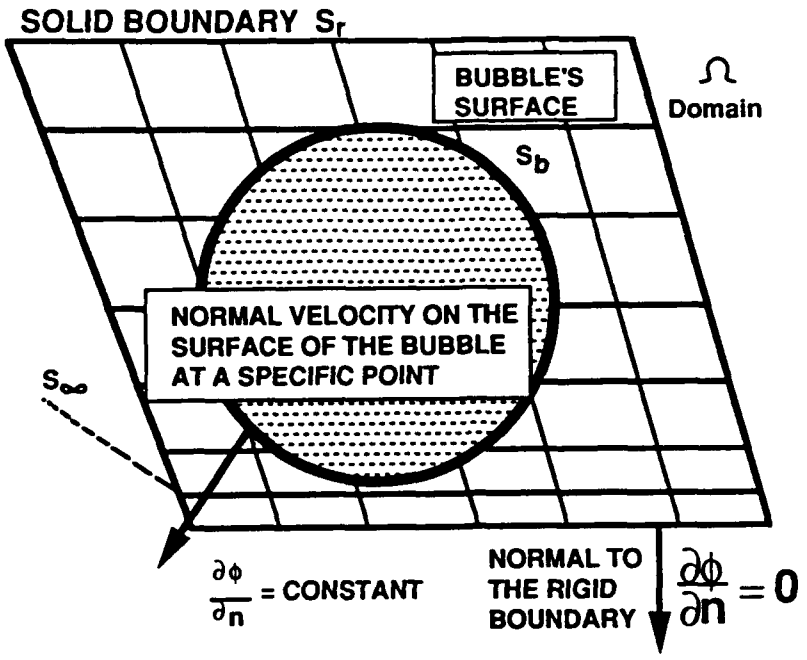

Figure 1. Definition of the Physical Problem.

The physical problem and the assumptions described previously can be stated in mathematical terms. The resulting mathematical formulation consists of two coupled equations, one derived from conservation of momentum and the other from the assumptions of irrotational flow and conservation of mass. Under the assumptions stated, these fundamental equations take the form of Bernoulli's equation and Laplace's equations. The solution of these two coupled equations is the basis of the computational model.

The first assumption is that the liquid is incompressible so that the divergence of the velocity vector is zero. This result derives from the conservation of mass equation and is as follows:

$$\nabla \cdot \underline{u} = 0. \tag{1}$$

For irrotational flow, the curl of the velocity field is zero,

$$\nabla \times \underline{u} = 0. \tag{2}$$

The previous expression is only satisfied when the velocity $\underline{u}$ is a function of the potential

$$\underline{u} = \nabla \phi . \tag{3}$$

Combining Equations 1 and 3 yields Laplace's equation to be satisfied in the domain Ω occupied by the fluid,

$$\nabla^2 \phi = 0. \tag{4}$$

The boundary conditions under which the equation must be solved are as follows:

$$\frac{dr}{dt} = \nabla \phi \quad \text{on } S_b , \tag{5}$$

$$\phi \rightarrow 0 \qquad |\underline{r}| \rightarrow \infty , \tag{6}$$

$$\frac{\partial \phi}{\partial n} = \nabla \phi \cdot n = 0 \quad \text{on } S_r , \tag{7}$$

where $\underline{r}$ is the position vector of a generic field point. The pressure in the liquid is given by Bernoulli's equation in the following:

$$\frac{\partial \phi}{\partial t} + \frac{u^2}{2} + \frac{P}{\rho} + gz = \frac{P_\infty}{\rho} , \tag{8}$$

where ρ is the liquid density, g is acceleration of gravity, and z is the vertical component of the position vector $\underline{r}$. In Equation 8, P_∞ denotes the pressure at a large distance from the bubble on the plane z=0. Insertion of the total derivative $d\phi/dt = \partial\phi/\partial t + u \cdot \nabla\phi = \partial\phi/\partial t + u^2$ into Equation 8 gives the following:

$$\frac{d\phi}{dt} = \frac{u^2}{2} + \frac{P}{\rho}\infty - \frac{P}{\rho} - gz . \tag{9}$$

The dynamic boundary condition on the surface of the bubble requires the liquid pressure to equal the internal pressure of the gas P_g. With this, integration in time of the expression in Equation 9 gives a boundary condition on the bubble's surface for the potential. Furthermore, the tangential derivatives of the potential on the bubble's surface can be determined from Equation 9. The remaining quantities to be determined are the gradient of the potential normal to the surface on the bubble and the internal gas pressure. Thus, Equations 4, 9, and the boundary conditions stated in Equations 5–7 form the basis for the current computational

model. The sections to follow will describe the mathematical model required for the solution of these two coupled equations under the boundary conditions prescribed.

One of the terms requiring further consideration in the conservation of momentum equation is the pressure at points on the surface of the bubble. Here, the pressure must equal the sum of the internal gas pressure and a surface tension component. For explosion bubbles, the surface tension component has been shown to be of little importance for most cases of explosion bubble dynamics (Wilkerson 1989, 1990). However, for cavitation and gas bubbles, this component can be of importance. The relation for the pressure on the surface of an explosion bubble can be written as follows:

$$P = P_g \ , \tag{10}$$

where P_g is the internal gas pressure of the bubble. This pressure, P_g, must be determined from an equation of state. After the initial gas pressure is found, the internal gas pressure can be updated from the ratio of volumes as follows:

$$P_g = P_{go}\left(\frac{V_i}{V_c}\right)^{\gamma} , \tag{11}$$

where V_c is the current volume V_i is the initial volume, P_{go} is the initial internal gas pressure, and γ is the adiabatic constant which depends on the explosive type. The adiabatic law is approximate because the thermal penetration length in the bubble is much smaller than its radius. The adiabatic constant γ has been empirically extracted from underwater explosive testing.

Effective initial conditions are needed to determine P_{go} and the initial radius. As a first guess for the initial internal bubble gas pressure P_{go}, the mass of the explosive charge can be converted directly into a high pressure gas, and an adiabatic pressure volume relation can be used thereafter. However, due to the finite time required for the explosive to convert into a gas, the effects of compressibility in the fluid, and the small expansion of the gas products during the chemical reaction, this assumption results in a poor initial condition for the pressure and the initial bubble radius. The resulting calculation for predicting bubble radius and bubble periods has unacceptably high errors when compared to experimental results.

Recently, Chahine (1989) has shown that with experimental knowledge of minimum and maximum bubble radii for an explosive type, the Rayleigh-Plesset equation can be integrated, yielding more consistent initial conditions for the internal pressure at a given radius. The relation discussed in Chahine (1989) is based on the Rayleigh-Plesset equation or spherical bubbles and some empirical data from explosion bubble experimentation. The principles of the expression are given here. The Rayleigh-Plesset equation is as follows:

$$\rho\left[R\ddot{R} + \frac{3}{2}\dot{R}^2\right] = P_{go}\left(\frac{R_o}{R}\right)^{3\gamma} - P_a \,, \tag{12}$$

where R is the radius and P_a is the ambient pressure far away from the bubble at the initial depth of its center. Here, the dots denote derivatives with respect to time. When the ambient pressure P_a is constant, Equation 12 is integrable when written in the following form (Plesset 1949):

$$\frac{\rho}{2}\left(\frac{d}{dR}(R^3\dot{R}^2)\right) = P_g(R_o^{3\gamma})R^{2-3\gamma} - P_a R^2 . \tag{13}$$

Integrating Equation 13 and allowing the current radius R to equal the maximum bubble radius, R_o to equal the minimum or initial bubble radius, and the corresponding velocities to equal zero, yields the following relation for the initial bubble pressure:

$$P_{go} = \frac{P_a(\gamma-1)\,(1-\alpha^{-3})}{1-\alpha^{3(\gamma-1)}} \,, \tag{14}$$

where $\alpha = R_{min}/R_{max}$ is the ratio of minimum to maximum bubble radii. For a more detailed derivation of Equation 14, see Chahine (1989). Data for the ratio α can be found for a number of explosive types in experimental studies (Snay, Goertner, and Price 1952). This relation applies at large depths where an explosion bubble remains spherical. Since bubbles are approximately spherical during their growth in shallow water as well, this relation applies approximately by adjusting P_a. Therefore, the remaining problem is how to obtain the initial radius. The initial radius can be determined from one of two methods. One method involves an empirical relation for the pressure P_{go} based on the weight, explosive type, and volume of the charge. Once such accepted pressure relation for TNT is (Cole 1948) as follows:

$$P_{go} = 7.8\left(\frac{W}{V}\right)^{\gamma}, \tag{15}$$

where W is the mass of TNT in grams, V is the volume in cm^3, P_{go} is the pressure in kilobars, and γ is the adiabatic constant for TNT, which is approximately 1.25. This relation is valid for $P < 4{,}500$ lb/in^2 pressure. The previous relation has been confirmed for TNT underwater explosive by Wilkerson (1989, 1990).

Another method of determining the initial pressure is based on an empirical relation for the maximum radius and the previous expression relating the minimum to maximum bubble radii α. This approach requires an estimation of R_{max}. This can be determined on the basis of empirical rules for explosion bubbles. This rule came from a dimensional analysis argument which related explosive energy to bubble energy. While the exact roots of the expressions given here are difficult to trace, the formula for maximum bubble radius of an explosive charge can be deduced from the following argument. The energy of the explosive charge E is proportional to the product of the maximum volume of water displaced at a given hydrostatic pressure times a constant K as follows:

$$E = KPV. \tag{16}$$

The energy of the charge is proportional to the weight of the charge W, the hydrostatic pressure is proportional to the depth Z plus the ambient pressure at the fluid's surface (e.g., $D = Z + 33$ where all depths are in feet), and the maximum volume is proportional to the maximum radius of the bubble cubed R^3_{max}. (At a depth of 33 ft, the hydrostatic head equals approximately 1 atmosphere of pressure.) From these relations, an expression for the maximum bubble radius can be written as follows:

$$R_{max} = J\left(\frac{W}{Z + 33}\right)^{1/3}, \tag{17}$$

where J is a constant to be determined from experimental results. The constant J has been determined for a number of explosive types at deep depths from underwater explosion experimentation (Swift and Decius 1950).

The remaining quantities to be prescribed for the boundary integral method are the initial values of the velocity and potential. The velocity is assumed to vanish, $u = 0$ at $t = 0$. Since the physically significant quantity is $u = \nabla\phi$, ϕ can be taken to vanish initially.

To simplify the validation of the codes, it is convenient to use scaling factors, making the results nondimensional. The parameters chosen are consistent with the thinking used to determine the initial conditions for the model. P_a = hydrostatic plus atmospheric pressure at the assumed depth of the initial bubble (e.g., an explosive at a 33-ft depth would have a P_a of approximately two atmospheres); ρ is the density of the fluid; and R_{max} is given by Equation 17 and corresponds to the observed maximum radius of an explosion bubble in the free field (the empirical rule just derived for maximum bubble radius in the absence of gravity). Using these three parameters, scale factors for time T_s, length L_s, and mass M_s were defined. They are as follows:

$$\begin{aligned} T_s &= R_{max}\sqrt{\rho / P_a}\,, \\ L_s &= R_{max}\,, \\ M_s &= \rho R_{max}^3\,. \end{aligned} \tag{18}$$

Dimensionless pressures are defined by P/P_a. In terms of these fundamental quantities, the mathematical model may be written as follows:

$$\begin{aligned} &\nabla^2\phi = 0\,, \\ &\frac{d\phi}{dt} = \frac{u^2}{2} + 1 - P_g - \frac{z}{F_r}\,, \\ &P_g = P_{go}\left(\frac{V}{V_c}i\right)^{\gamma}\,, \end{aligned} \tag{19}$$

where all quantities are dimensionless, and the Froude number is defined by $F_r = P_a/\rho g L_s = d/R_{max}$, where d is the depth of the charge. It is seen from Equation 19 that for small values of F_r, the effect of gravity is important, while it is negligible for $F_r >> 1$. In particular, the limit in which the Rayleigh-Plesset equation is appropriate is obtained for $F_r \to \infty$.

The boundary integral formulation for the solution of Laplace's equation is based on the use of Green's second identity which reduces a volume integral to a surface integral. The remaining surface integral is discretized, yielding a linear algebraic system for the gradient of the potential normal to the boundaries. The starting point of the boundary integral method is Green's second identity as follows:

$$\int_V (\phi \nabla^2\psi - \psi\nabla^2\phi)\, dV = \int_V (\phi \frac{\partial\psi}{\partial n} - \psi \frac{\partial\phi}{\partial n})\, dS\,, \tag{20}$$

which is valid for any pair of sufficiently smooth functions ϕ and ψ. In the present approach, ϕ is taken to be the velocity potential discussed in Section 2.2, and ψ is taken to be the free space Green's function for Laplace's equation as follows:

$$\psi = \frac{1}{|\underline{r} - \underline{R}|}. \tag{21}$$

Physically, this represents the field at position $\underline{R}$, generated by a source of intensity 4π placed at $\underline{r}$. This function satisfies an equation of the following form:

$$\nabla^2\psi = -\lambda\delta(\underline{r} - \underline{R})\,, \tag{22}$$

where the Laplacian is with respect to the variable $\underline{R}$. Here, $\lambda = 4\pi$ if $\underline{R}$ is internal to the domain Ω. When $\underline{R}$ is located on the boundary (in particular, on the bubble's surface S), λ equals the solid angle under which the domain Ω is viewed from $\underline{R}$. It is important to note that λ must be evaluated for the actual discretized shape of the boundary rather than for the exact one; otherwise, incorrect numerical results would be found. Substitution of Equations 21 and 22 into Equation 20 yields the following:

$$\lambda\phi(\underline{R}) = \int_S \left(\left[\frac{1}{|\underline{r} - \underline{R}|} \right] \frac{\partial\phi}{\partial n_r}(\underline{r}) - \phi(\underline{r}) \frac{\partial}{\partial n_r} \left[\frac{1}{|\underline{r} - \underline{R}|} \right] \right) dS\,. \tag{23}$$

The model updating in this formulation involves the time integration of Equation 9 and the tracking of the bubble's surface with time. In order to follow the bubble's shape, an accurate estimation of the bubble's surface velocity, based on the tangential and normal velocity, must be determined. Inaccuracies in the estimation of the bubble's velocity must be determined.

Inaccuracies in the estimation of the bubble's velocity will add to instabilities in the numerical solution. As a first attempt, a first-order finite difference scheme was used. However, the resulting integration required a small time step and caused the overall computation to be too long. Therefore, a combination of an explicit and implicit finite difference scheme was used to help stabilize the bubble code's time integration and model updating. The combination of the two expressions resulted in a method accurate to the second order and far more stable numerically. The method used has the following form:

$$x_{i+1} = x_i + (\dot{x}_i + \dot{x}_{i+1})\Delta t/2 \,, \tag{24}$$

for each of the Cartesian coordinates, and

$$\phi_{i+1} = \phi_i + (\dot{\phi}_i + \dot{\phi}_{i+1})\Delta t/2 \tag{25}$$

for updating the potential. Other possible methods to help stabilize the time integration also exist. One such method is given in Chahine, Perdue, and Tucker (1988). In this approach, a term for artificial viscosity is included in Equation 9. This term accomplishes the same result as the combination of the finite difference schemes. Another possibility would be to use a higher-order predictor corrector method. This method would significantly increase computation time, thereby defeating some of the appeal of the current method.

For a single degree of freedom system, namely, a spherically symmetric system, Equation 12 can be integrated directly for a solution. Such solutions have been shown in good agreement with experimental and other numerical studies (Wilkerson 1989). For an axisymmetric configuration, it is necessary to break up the bubble's boundary into discrete segments. For the current development, the initial axisymmetric discretization consists of equally spaced, straight line segments around the bubble's shape. This initial discretization, shown in Figure 2, shows how the bubble's shape can be approximated by n straight line segments with n + 1 nodes. The geometry is based on a cylindrical coordinate system (r, z,θ) where θ is the counterclockwise rotation about the z axis.

For the axisymmetric formulation, the vectors $\underline{r}$ and $\underline{R}$ locating field points on boundaries are given by the following relations:

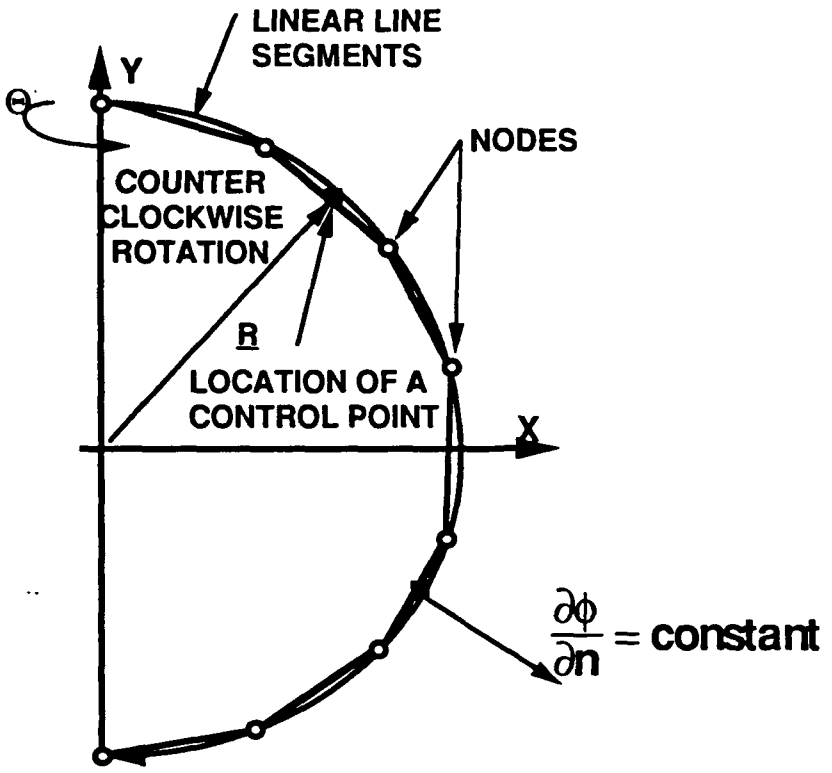

Figure 2. Axisymmetric Discretization (Cylindrical Coordinates).

$$\underline{r} = [r\cos(\theta), r\sin(\theta), z] \ ,$$
$$\underline{R} = [R, 0, Z] \ . \qquad (26)$$

The 3-D formulation offered a number of alternatives with regards to the initial gridding. Some of the possibilities included three-noded triangles, rectangular patches, or other shaped elements. For the current numerical model, three-noded triangular patches were used. The first level of discretization for the 3-D model is based on the initial shape of an icosahedron. This shape consists of 20 equilateral triangles and 12 nodes, all of which lie on the surface of a sphere. This initial level of discretization can be improved by breaking up each of the original triangles into smaller triangles. With each additional level of refinement, the coarseness of the original icosahedron shape can be gradually improved to more closely approximate a near-spherical shape. The process of level refinement is shown graphically in Figure 3.

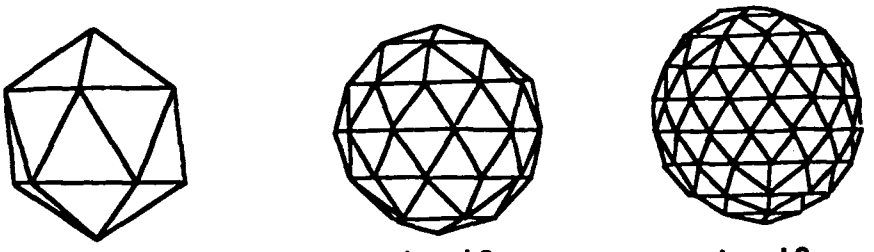

Level 1
20 Elements
12 Nodes

Level 2
80 Elements
42 Nodes

Level 3
180 Elements
92 Nodes

Figure 3. First Three Levels of Discretization for Triangles.

A field point anywhere on the surface of an element can be defined by the position vector $\underline{r}$ as follows:

$$\underline{r} = \sum_{i=1}^{3} N_i x_i i + \sum_{i=1}^{3} N_i y_i j + \sum_{i=1}^{3} N_i z_i k \ , \tag{27}$$

where N_i is the shape function for a standard triangular element, x_i, y_i, z_i are the nodal coordinates, and i, j, k the Cartesian coordinate system's unit vectors. Since these relationships apply to any linear quantity on the surface of the element, a similar method can be applied for interpolating the potential and gradient of the potential on the surface in terms of the shape functions and the nodal values of these quantities. These relations are as follows:

$$\phi = \sum_{i=1}^{3} N_i \phi_i \ , \tag{28}$$

$$\left(\frac{\partial\phi}{\partial n}\right) = \sum_{i=1}^{3} N_i \left(\frac{\partial\phi}{\partial n}_i\right), \tag{29}$$

where N_i is the same shape function given in Equation 27, ϕ and $\partial\phi/\partial n$ are the interpolated potential and gradient of the potential anywhere on the surface of the element, and ϕ_i and $\partial\phi_i/\partial n$ are the nodal values of the potential and gradient of the potential. The global coordinates of the $\underline{R}$ vector are as follows:

$$\underline{R}_i = R_{xi}\,i + R_{yi}\,j + R_{zi}\,k\,, \tag{30}$$

where i refers to the global node number.

3. RESULTS

Comparisons were made with the axisymmetric formulation for free-field bubble jetting. The present axisymmetric code has been shown to be in good agreement with physical phenomena and other numerical approaches for the calculation of bubble jet velocities by Wilkerson (1989). Further, direct comparisons with the axisymmetric code of Oguz and Prosperetti (1989) were also made.

The first comparison is between the axisymmetric code and the first-order 3-D code. This comparison uses the results from a calculation for a 1-lb charge of TNT with a total hydrostatic head of 33 ft. Under these conditions, there is a strong influence of gravity, and the bubble should form a jet firing the collapse phase of its first pulsation. Plots comparing velocity and displacement of the north and south poles of the bubble are provided. Figure 4 compares the absolute velocity of the bubble's north pole from the two calculations. Similarly, Figure 5 compares the absolute velocity of the bubble's south poles. It is important to note that these calculations were made using dimensionless quantities. Note that for the dimensionless units used, the fundamental velocity is $\sqrt{P_a/\rho}$ = 33.0 ft/s. Therefore, the velocities from the south pole, where the bubble jet is formed during the late stages of collapse, are quite large.

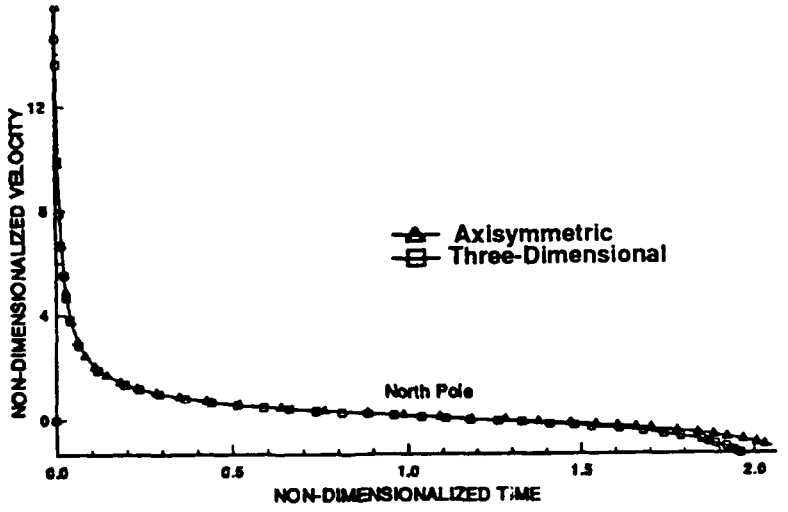

Figure 4. Comparison of Bubble North Pole Surface Velocity as Computed by the Axisymmetric and 3-D Bubble Codes.

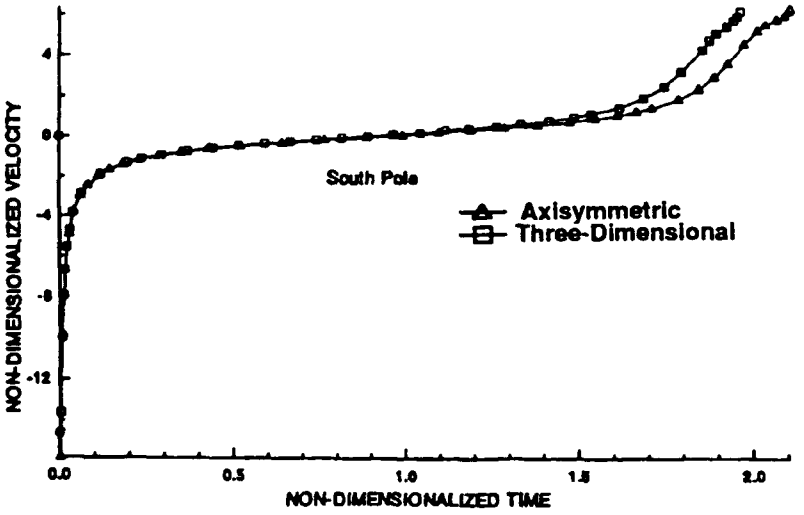

Figure 5. Comparisons of Bubble South Pole Surface Velocity as Computed by the Axisymmetric and 3-D Bubble Codes.

Similar plots comparing the north and south pole displacements in the two calculations are given in Figures 6 and 7, respectively. Theoretically, the displacements at bubble maximum in Figures 6 and 7 should be close to ±1.0 when using nondimensional variables. However, due to small inaccuracies in the method's ability to predict the bubble's volume in these calculations, the bubble slightly overexpands. This was expected due to the increase in the bubble's pressure which is affected by the volume calculation.

Figure 8 shows a comparison between the bubble shape predicted by first-order 3-D code and the axisymmetric code for the same free-field bubble dynamics simulations. In the figure, the 3-D code shows good agreement in predicting the broad, smooth bubble jet typical of gravity induced bubble jetting. The 3-D code used a level four discretization, and the axisymmetric code uses nine segments. The crude discretization applied in the axisymmetric calculation was used in order to give a comparable representation of the bubble's surface between the 3-D and the axisymmetric calculation.

In order to show the potential for 3-D calculations with the boundary integral method, a series of calculations with infinite rigid plates at various angles is provided. The calculations include the effects of both gravity and the nearby wall. The nearby wall is simulated by use of an image bubble. The figures include an infinite plate directly over the bubble (Figure 9), a plate at a 45° angle above the bubble (Figure 10), a vertical plate adjacent to the bubble (Figure 11), a plate at 45° angle below the bubble (Figure 12), and a plate directly beneath the bubble (Figure 13). All of the calculations performed were at a standoff of one bubble radius for the infinite wall and all calculations used the same Froude number. The maximum bubble radius was estimated from a free field calculation and is given by Equation 17. The Froude number is a nondimensional ratio of inertia to gravity forces $Fr = V^2/gL$. These calculations are for a Froude number of 8.6. The calculation of the Froude number was based on $Fr = V^2/gL = L_s/gT_s^2$. Additionally, the initial conditions duplicate a 1-lb TNT explosive charge with a total hydrostatic head of 33 ft. In these calculations, the effects of gravity are fairly strong. All the figures are made using level four discretization. In Figure 9, the effects of gravity and attraction to the wall act in the same direction. As expected, the jet is attracted toward the wall and is somewhat sharper and has a higher velocity than of the free field calculation (see Figure 8), where the effects of gravity are isolated. It is important to note that this calculation could have been made with the axisymmetric code. However, the calculations

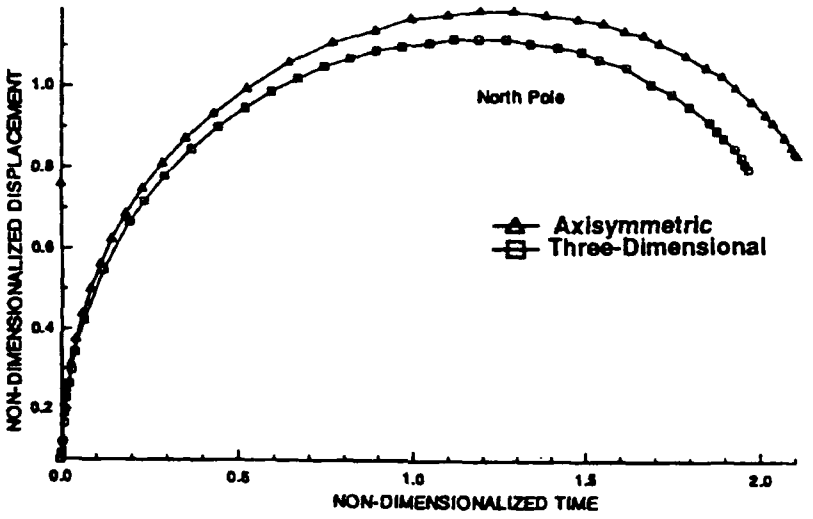

Figure 6. Comparisons of Bubble North Pole Surface Displacements as Computed by the Axisymmetric and 3-D Bubble Codes.

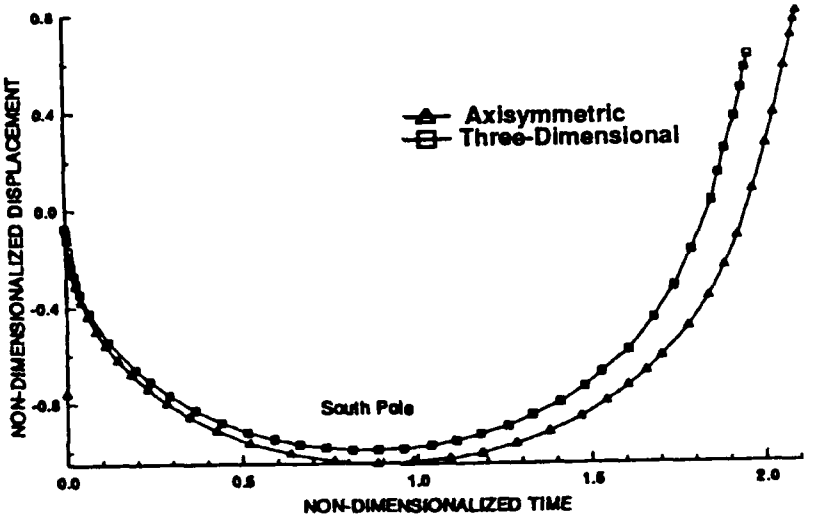

Figure 7. Comparison of Bubble South Pole Surface Displacements as Computed by the Axisymmetric and 3-D Bubble Codes.

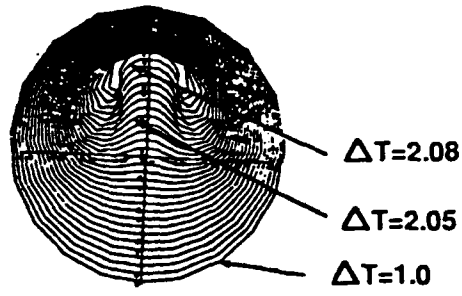

Axisymmetric Calculation

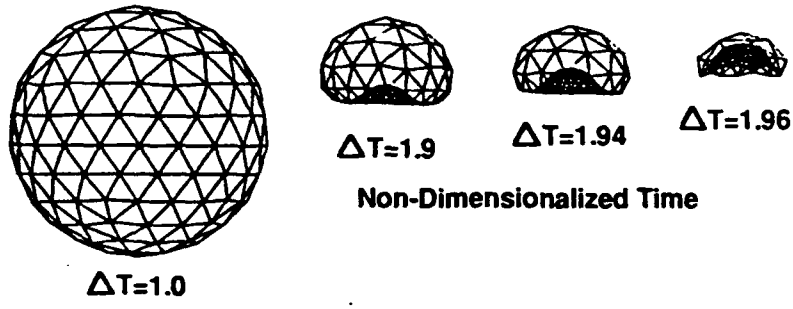

Three-Dimensional Calculation

Figure 8. Predicted Bubble Shapes as Computed by the Axisymmetric and the 3-D Bubble Codes.

Horizontal Rigid Plate Above Bubble

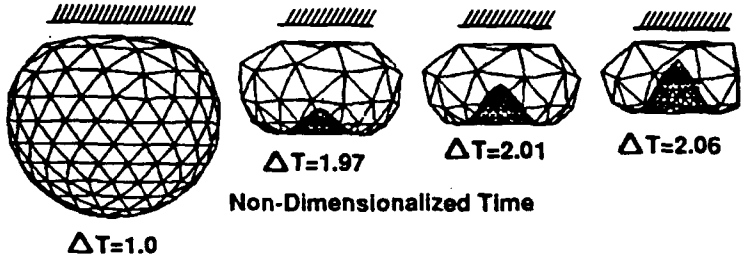

Figure 9. The Calculation of an Explosion Bubble's Collapse Near an Infinite Rigid Boundary Using the 3-D Bubble Code.

45° Inclined Rigid Plate Above Bubble

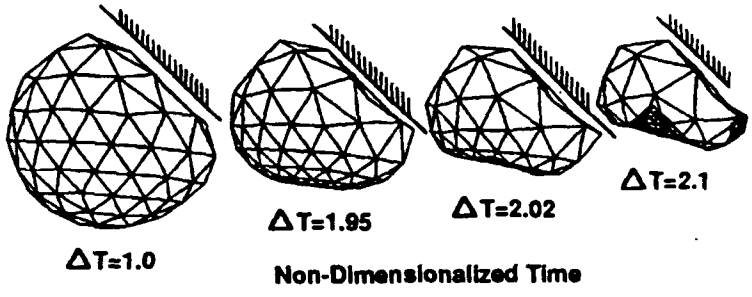

Figure 10. The Calculation of an Explosion Bubble's Collapse Near an Infinite Rigid Boundary Using the 3-D Bubble Code.

Vertical Rigid Plate Along Side Bubble

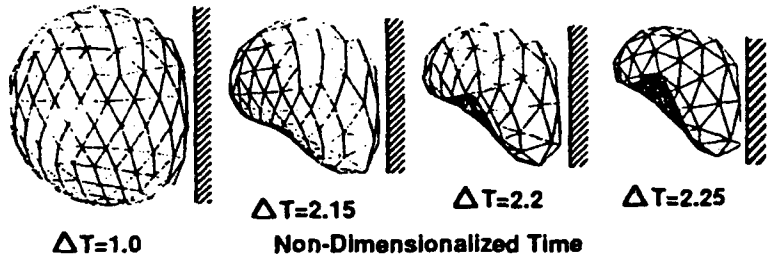

Figure 11. The Calculation of an Explosion Bubble's Collapse Near an Infinite Rigid Boundary Using the 3-D Bubble Code.

45° Inclined Rigid Plate Below Bubble

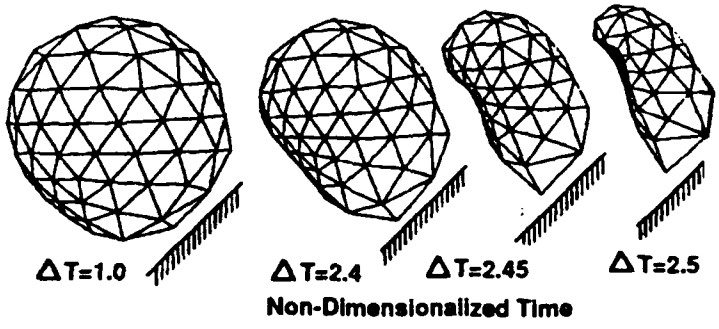

Figure 12. The Calculation of an Explosion Bubble's Collapse Near an Infinite Rigid Boundary Using the 3-D Bubble Code.

Horizontal Rigid Plate Below Bubble

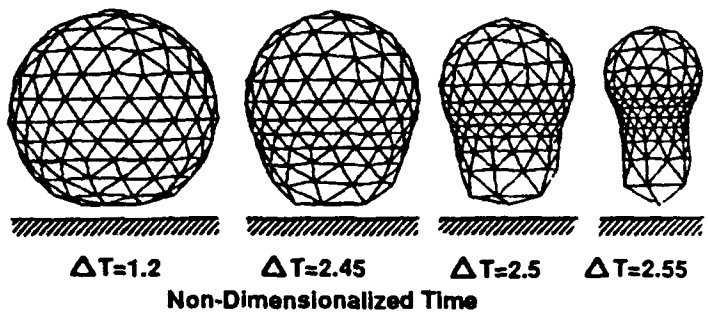

Figure 13. The Calculation of an Explosion Bubble's Collapse Near an Infinite Rigid Boundary Using the 3-D Bubble Codes.

with the inclined and vertical plate are not axisymmetric and in the interest of consistency; all of the figures presented in this section are made using a full 3-D calculation. Figure 10 shows the influence of a 45° inclined plate above the bubble. In this simulation, the influence of the plate on the late stages of bubble jet development are evident. The simulations are sufficient for the determination of jet direction and magnitude of its velocity. Therefore, this method can be said to be well suited for the study of bubble jetting in a strong gravity field in the presence of nearby objects. This is of importance from a military standpoint for obvious reasons. In Figures 11 and 12, the declining influence of the infinite plate on bubble jet directionality can be clearly seen. Finally, in Figure 13, gravity and the influence of the rigid plate oppose one another. The calculation indicates the formation of a ring jet around the lower circumference of the bubble. Similar calculations with bubbles between two infinite plates, where the attractive force of the plates oppose one another, have been made in axyismmetric conditions by Kucera and Blake (1989), with a 3-D code by Chahine (1982), and was observed by Chahine (1989). In these calculations, the bubble forms a ring jet about its circumference which eventually separates the bubble, in an hourglass fashion, into two bubbles. Both calculations are similar insofar that they are axisymmetric in nature and the two forces influencing bubble collapse oppose each other.

4. SUMMARY

The boundary integral method was used to develop axisymmetric and 3-D numerical solutions for explosion bubble dynamics studies. These formulations were adapted specifically for studies involving underwater explosion bubbles. A number of bubble codes have been developed and are discussed during the current formulation. The validity and some of the limitations were established through comparisons with previously developed codes.

The current effort offers a number of alternatives for the calculation of bubble dynamics. The 3-D code was unique in its numerical solution for the integral evaluation (Wilkerson 1990). Further, the method developed used a consistent finite element solution for interpolating values of the potential and the velocities on each triangular element.

Future efforts using this boundary integral approach will be centered around understanding and controlling inherent instabilities in the solution process which are typically found in underwater explosion bubble dynamics.

5. REFERENCES

Bevir, M. K., and P. J. Fielding. "Numerical Solution of Incompressible Bubble Collapse With Jetting." Moving Boundary Problems in Heat Flows and Diffusion, Clarendon Press, 1974.

Benjamin, T. B., and A. T. Ellis. "Cavitation: The Collapse of Cavitation Bubbles and the Pressures Thereby Produced Against Solid Boundaries." Philosophical Transactions of the Royal Society of London, vol. 260, pp. 221–240, 1966.

Blake, J. R., and D. C. Gibson. "Growth and Collapse of a Vapour Cavity Near a Free Surface." Journal of Fluid Mechanics, vol. 111, pp.123–140, February 1981.

Blake, J. R., B. B. Taib, and G. Doherty. "Transient Cavities Near Boundaries Part 1. Rigid Boundary." Journal of Fluid Mechanics, vol. 170, pp. 479–497, March 1986.

Chahine, G. L. "Interaction Between and Oscillating Bubble and a Free Surface." American Society of Mechanical Engineers, 1977.

Chahine, G. L. "Experimental and Asymptotic Study of Nonspherical Bubble Collapse." Applied Scientific Research, no. 38, pp.187–197, 1982.

Chahine. G. L., T. O. Perdue, and C. B. Tucker. "Interaction Between an Underwater Explosion Bubble and a Solid Submerged Body." Tech Report 86029-1, Traycor Hydronautics, Inc., 1988.

Chahine, G. L. "A Numerical Model for Three-Dimensional Bubble Dynamics in Complex Flow Configurations." Tech Report 6.02-2, ATTC Conference, Newfoundland, September 1989.

Chapman, R. B., and M. S. Plesset. "Nonlinear Effects in the Collapse of a Nearly Spherical Cavity in a Liquid." Journal of Basic Engineering, pp. 142–146, March 1972.

Cole, R. H. Underwater Explosions. Princeton, New Jersey, 1948.

Guerri, L., G. Lucca, and A. Prosperetti. "A Numerical Method for the Dynamics of Nonspherical Cavitation Bubbles." JPL, vol. 82-7, pp. 175–181, 1992.

Hammit, F. G. "Observations of Cavitation Damage in a Flowing System." Transactions of the American Society of Mechanical Engineers Journal of Basic Engineering, vol. 85, pp. 347, 1963.

Knapp, R. T., and A. Hollander. "Laboratory Investigation of the Mechanism of Cavitation." Transactions of the American Society of Mechanical Engineers, vol. 70, pp. 419, 1948.

Knapp, R. T. "Accelerated Field Tests of Cavitation Intensity." Transactions of the American Society of Mechanical Engineers," vol. 80, pp. 91, 1958a.

Knapp, R. T. "Recent Investigations of the Mechanics of Cavitation Damage." Transactions of the American Society of Mechanical Engineers, vol. 77, pp. 1045, 1958b.

Kucera, A., and J. R. Blake. "Approximate Methods for Modeling Cavitation Bubbles Near Boundaries," University of Wollongong, Wollongong, Australia, March 1989.

Lamb, H. Hydrodynamics. New York: Dover Publications, 1945.

Lord Rayleigh. "On the Pressure Developed in a Liquid During the Collapse of a Spherical Cavity." Phil. Mag, vol. 34, pp. 94–98, 1917.

Oguz, H. N., and A. Prosperetti. "Bubble Entrainment by the Impact of Drops on Liquid Surfaces." Journal Fluid Mechanics, 1989.

Perdue, T. O'Brian. "A Three-Dimensional Numerical Simulation of Bubble Growth and Collapse Near A Rigid Boundary in the Presence of Gravity." Master of Science Thesis, University of Maryland, 1988.

Plesset, M. S. "The Dynamics of Cavitation Bubbles." American Society of Mechanical Engineering Journal of Applied Mechanics, vol. 16, pp. 277–282, September 1949.

Plesset, M. S., and R. B. Chapman. "Collapse of an Initially Spherical Vapour Cavity in the Neighborhood of a Solid Boundary." Journal of Fluid Mechanics, vol. 47, Part II, pp. 283–290, 1971.

Snay, H. G., J. F. Goertner, and R. S. Price. "Small Scale Experiments to Determine Migration of Explosion Gas Globes Towards Submarines." Report 2280, Naval Ordnance Laboratory, 1952.

Swift, E., and J. C. Decius. "Measurement of Bubble Pulse Phenomena, III Radius and Period Studies." Underwater Explosion Research, vol. II-The Gas Globe, ONR, 1950.

Taylor, G. I. "Vertical Motion of a Spherical Bubble and the Pressure Surrounding It." Underwater Explosion Research, vol. II-The Gas Globe, ONR, 1950.

Taylor, G. I., and R. M. Davies. "The Motion and Shape of the Hollow Produced by an Explosion in a Liquid." Underwater Explosion Research, vol. II-The Gas Globe, ONR, 1950.

Wilkerson, S. A. "Boundary Integral Technique for Explosion Bubble Collapse Analysis." American Society of Mechanical Engineering Energy-Sources Technology Conference and Exhibition, Publication no. 89-OCN-2, Houston, TX, 22–25 January 1989.

Wilkerson, S. A. "A Boundary Integral Approach to Three-Dimensional Underwater Explosion Bubbles Dynamics." Ph.D. Thesis, The Johns Hopkins University, May 1990.

No. of Copies Organization

2 Administrator
Defense Technical Info Center
ATTN: DTIC-DDA
Cameron Station
Alexandria, VA 22304-6145

1 Commander
U.S. Army Materiel Command
ATTN: AMCAM
5001 Eisenhower Ave.
Alexandria, VA 22333-0001

1 Commander
U.S. Army Laboratory Command
ATTN: AMSLC-DL
2800 Powder Mill Rd.
Adelphi, MD 20783-1145

2 Commander
U.S. Army Armament Research,
Development, and Engineering Center
ATTN: SMCAR-IMI-I
Picatinny Arsenal, NJ 07806-5000

2 Commander
U.S. Army Armament Research,
Development, and Engineering Center
ATTN: SMCAR-TDC
Picatinny Arsenal, NJ 07806-5000

1 Director
Benet Weapons Laboratory
U.S. Army Armament Research,
Development, and Engineering Center
ATTN: SMCAR-CCB-TL
Watervliet, NY 12189-4050

(Class. only)1 Commander
U.S. Army Rock Island Arsenal
ATTN: SMCRI-TL/Technical Library
Rock Island, IL 61299-5000

1 Director
U.S. Army Aviation Research
and Technology Activity
ATTN: SAVRT-R (Library)
M/S 219-3
Ames Research Center
Moffett Field, CA 94035-1000

1 Commander
U.S. Army Missile Command
ATTN: AMSMI-RD-CS-R (DOC)
Redstone Arsenal, AL 35898-5010

No. of Copies Organization

1 Commander
U.S. Army Tank-Automotive Command
ATTN: ASQNC-TAC-DIT (Technical
Information Center)
Warren, MI 48397-5000

1 Director
U.S. Army TRADOC Analysis Command
ATTN: ATRC-WSR
White Sands Missile Range, NM 88002-5502

1 Commandant
U.S. Army Field Artillery School
ATTN: ATSF-CSI
Ft. Sill, OK 73503-5000

(Class. only)1 Commandant
U.S. Army Infantry School
ATTN: ATSH-CD (Security Mgr.)
Fort Benning, GA 31905-5660

(Unclass. only)1 Commandant
U.S. Army Infantry School
ATTN: ATSH-CD-CSO-OR
Fort Benning, GA 31905-5660

1 WL/MNOI
Eglin AFB, FL 32542-5000

Aberdeen Proving Ground

2 Dir, USAMSAA
ATTN: AMXSY-D
AMXSY-MP, H. Cohen

1 Cdr, USATECOM
ATTN: AMSTE-TC

3 Cdr, CRDEC, AMCCOM
ATTN: SMCCR-RSP-A
SMCCR-MU
SMCCR-MSI

1 Dir, VLAMO
ATTN: AMSLC-VL-D

10 Dir, USABRL
ATTN: SLCBR-DD-T

No. of
Copies Organization

2 Commander
U.S. Army Armament Research,
Development, and Engineering Center
ATTN: SMCAR-TD,
V. Linder
T. Davidson
Picatinny Arsenal, NJ 07806-5000

1 Commander
Production Base Modernization Activity
U.S. Army Armament Research,
Development, and Engineering Center
ATTN: AMSMC-PBM-K
Picatinny Arsenal, NJ 07806-5000

1 Commander
U.S. Army Belvoir RD&E Center
ATTN: STRBE-JBC, C. Kominos
Fort Belvoir, VA 22060-5606

2 Commander
U.S. Army Laboratory Command
Harry Diamond Laboratories
ATTN: SLCHD-TS-NT, A. Frydman
2800 Powder Mill Road
Adelphi, MD 20783-1197

1 Commander
U.S. Army Laboratory Command
ATTN: AMSLC-TD, R. Vitali
Adelphi, MD 20783-1145

1 Commander
U.S. Army Missile Command
ATTN: AMSMI-RD, W. McCorkle
Redstone Arsenal, AL 35898

3 Commander
U.S. Army Armament Research,
Development, and Engineering Center
ATTN: SMCAR-FSA-M,
R. Botticelli
F. Diorio
SMCAR-FSA,
C. Spinelli
Picatinny Arsenal, NJ 07806-5000

No. of
Copies Organization

3 Project Manager
Advanced Field Artillery System
ATTN: COL Napoliello
LTC D. Ellis
G. DelCoco
Picatinny Arsenal, NJ 07806-5000

1 Commander
Watervliet Arsenal
ATTN: SMCWV-QA-QS, K. Insco
Watervliet, NY 12189-4050

1 Project Manager
SADARM
Picatinny Arsenal, NJ 07806-5000

2 Project Manager
Tank Main Armament Systems
ATTN: SFAE-AR-TMA, COL Hartline
SFAE-AR-TMA-MD, C. Kimker
Picatinny Arsenal, NJ 07806-5000

2 PEO-Armaments
ATTN: SFAE-AR-PM,
D. Adams
T. McWilliams
Picatinny Arsenal, NJ 07806-5000

1 Commander
DARPA
ATTN: J. Kelly
1400 Wilson Blvd.
Arlington, VA 22209

2 Director
U.S. Army Materials Technology
Laboratory
ATTN: SLCMT-MEC,
B. Halpin
T. Chou
Watertown, MA 02172-0001

1 Naval Research Laboratory
Code 6383
ATTN: I. Wolock
Washington, DC 20375-5000

No. of Copies	Organization
2	David Taylor Research Center ATTN: R. Rockwell W. Phyillaier Bethesda, MD 20054-5000
1	David Taylor Research Center Ship Structures and Protection Department Code 1702 ATTN: J. Corrado Bethesda, MD 20084
4	Office of Naval Technology ATTN: OCNR-20 OCNR-23 OCNR-232 OCNR-213 Ballston Center Towers #1, Rm 503 800 N. Quincy Street Arlington, VA 22217-5000
1	ODDR&E/Tactical Warfare ATTN: R. Menz The Pentagon Washington, DC 20301
10	ODDR&E/Chief of Naval Operations ATTN: OP-22 OP-225 OP-35 OP-353 OP-354 OP-374 OP-411 OP-71 OP-981 Technical Library Department of the Navy Washington, DC 20350
6	Commander Naval Sea Systems Command ATTN: SEA-55X, D. Bruder SEA-55X, B. McCarthy SEA-402 SEA-406 SEA-407 SEA-423 Department of the Navy Washington, DC 20362

No. of Copies	Organization
7	Commander David W. Taylor Research Center ATTN: Code 17 Code 172 Code 175, J. Sykes Code 175.1, Dr. B. Whang Code 175.2 , W. Conley P. Manny D. Hagar Bethesda, MD 20084
4	Office of Naval Research ATTN: Code 1132-SM Code 1132-P Code 1132-F Technical Library 800 North Quincy Street Arlington, VA 22217
6	The Naval Surface Warfare Center ATTN: D4 E231 E232 H14 R R10 10901 New Hampshire Avenue Silver Spring, MD 20903-5000
5	The Naval Surface Warfare Center ATTN: R10A, D. Phillips K. W. Reed R11, R. M. Doherty R14 R44, W. Szymczak 10901 New Hampshire Avenue Silver Spring, MD 20903-5000

No. of
Copies Organization

10 The Naval Surface Warfare Center
ATTN: U
U02
U08
U11, E. Johnson
U12, W. Hinckley
C. Smith
W. Walker
U20
U24
U31, Dr. C. McClure
10901 New Hampshire Avenue
Silver Spring, MD 20903-5000

4 Director
Defense Nuclear Agency
ATTN: Code SPSD,
Dr. T. Tsai
Dr. K. Goering
Code SPWE, C. McFarland
Technical Library
Washington, DC 20305

2 Pacific Northwest Laboratory
A Division of Battelle Memorial Institute
Technical Information Section
ATTN: M. Smith
M. Garnich
P.O. Box 999
Richland, WA 99352

2 Director
Sandia National Laboratories
Applied Mechanics Department
Division 8241
ATTN: C. Robinson
G. Benedetti
P.O. Box 969
Livermore, CA 94550-0096

1 Los Alamos National Laboratory
ATTN: D. Rabern
MEE-13, Mail Stop J-576
P.O. Box 1633
Los Alamos, NM 87545

No. of
Copies Organization

2 Institute for Advanced Technology
ATTN: T. Kiehne
H. Fair
4030-2 W. Braker Lane
Austin, TX 78759

2 Lawrence Livermore National
Laboratory
ATTN: B. Bowman
Technical Library
Livermore, CA 94550

4 Library of Congress
ATTN: Gift and Exchange Division
Washington, DC 20540

USER EVALUATION SHEET/CHANGE OF ADDRESS

This laboratory undertakes a continuing effort to improve the quality of the reports it publishes. Your comments/answers below will aid us in our efforts.

1. Does this report satisfy a need? (Comment on purpose, related project, or other area of interest for which the report will be used.) _____

2. How, specifically, is the report being used? (Information source, design data, procedure, source of ideas, etc.) _____

3. Has the information in this report led to any quantitative savings as far as man-hours or dollars saved, operating costs avoided, or efficiencies achieved, etc? If so, please elaborate. _____

4. General Comments. What do you think should be changed to improve future reports? (Indicate changes to organization, technical content, format, etc.) _____

BRL Report Number BRL-TR-3365 Division Symbol _____

Check here if desire to be removed from distribution list. ____

Check here for address change. ____

Current address: Organization _____
Address _____
_____

DEPARTMENT OF THE ARMY
Director
U.S. Army Ballistic Research Laboratory
ATTN: SLCBR-DD-T
Aberdeen Proving Ground, MD 21005-5066

OFFICIAL BUSINESS

BUSINESS REPLY MAIL
FIRST CLASS PERMIT No 0001, APG, MD

Postage will be paid by addressee.

Director
U.S. Army Ballistic Research Laboratory
ATTN: SLCBR-DD-T
Aberdeen Proving Ground, MD 21005-5066

NO POSTAGE NECESSARY IF MAILED IN THE UNITED STATES